IFIC/16-08
FTUV/16-0219

arXiv:1602.06112v1 [hep-ph] 19 Feb 2016

Updated determination of chiral couplings and vacuum condensates from hadronic τ decay data

Martín Gonzalez-Alonso,[a] Antonio Pich[b] and Antonio Rodríguez-Sánchez[b]

[a] IPN de Lyon, CNRS and Université Lyon 1, F-69622 Villeurbanne, France
[b] Departament de Física Teòrica, IFIC, Universitat de València – CSIC,
Apt. Correus 22085, E-46071 València, Spain,

Abstract

We analyze the lowest spectral moments of the left-right two-point correlation function, using all known short-distance constraints and the recently updated ALEPH $V-A$ spectral function from τ decays. This information is used to determine the low-energy couplings L_{10} and C_{87} of chiral perturbation theory and the lowest-dimensional contributions to the Operator Product Expansion of the left-right correlator. A detailed statistical analysis is implemented to assess the theoretical uncertainties, including violations of quark-hadron duality.

1 Introduction

The hadronic decays of the τ lepton provide very valuable information on low-energy properties of the strong interaction, allowing us to analyze important perturbative and non-perturbative aspects of QCD [1]. A very precise determination of the strong coupling can be extracted from the inclusive hadronic τ decay width [2–7], while the SU(3)-breaking corrections to the $\Delta S = 1$ decay width [8, 9] are very sensitive to the Cabibbo quark mixing $|V_{us}|$ [10, 11]. In this paper we are interested in the difference between the vector (V) and axial-vector (A) τ spectral functions, which gives a direct access to non-perturbative parameters related with the spontaneous chiral symmetry breaking of QCD [12–27]. A very detailed phenomenological study of the non-strange $V - A$ spectral function, using the 2005 release of the ALEPH τ data [28], was already done in Refs. [22–24]. The recent update of the ALEPH non-strange τ spectral functions [29] motivates an updated numerical analysis, based on the strategies developed in those references, which we present here. A comparison with other works available in the literature that employ different theoretical approaches will also be performed.

Compared to the 2005 ALEPH data set, the new public version of the ALEPH τ data incorporates an improved unfolding of the measured mass spectra from detector effects and corrects some problems [30] in the correlations between unfolded mass bins. The improved unfolding brings an increased statistical uncertainty near the edges of phase space. It has also reduced the number of bins in the spectral distribution, as a larger bin size has been adopted.

The starting point of our analysis is the two-point correlation function of the left-handed and right-handed quark currents:

$$\begin{aligned} \Pi^{\mu\nu}_{ud,LR}(q) &\equiv i \int d^4x\, e^{iqx}\, \langle 0|\, T\left(L^\mu_{ud}(x) R^{\nu\dagger}_{ud}(0)\right) |0\rangle \\ &= (-g^{\mu\nu} q^2 + q^\mu q^\nu)\, \Pi^{(1)}_{ud,LR}(q^2) + q^\mu q^\nu\, \Pi^{(0)}_{ud,LR}(q^2)\,, \end{aligned} \tag{1}$$

where $L^\mu_{ud}(x) \equiv \bar{u}(x)\gamma^\mu(1-\gamma_5)d(x)$ and $R^\mu_{ud}(x) \equiv \bar{u}(x)\gamma^\mu(1+\gamma_5)d(x)$. Owing to the chiral invariance of the massless QCD Lagrangian, this correlator vanishes identically to all orders in perturbation theory when $m_{u,d} = 0$. The non-zero value of

$$\Pi(s) \;\equiv\; \Pi^{(0+1)}_{ud,LR}(s) \;\equiv\; \Pi^{(0)}_{ud,LR}(s) + \Pi^{(1)}_{ud,LR}(s) = \frac{2 f_\pi^2}{s - m_\pi^2} + \overline{\Pi}(s) \tag{2}$$

originates in the spontaneous breaking of chiral symmetry by the QCD vacuum, which results in different vector and axial-vector two-point functions. Thus, $\Pi(s)$ is a perfect theoretical laboratory to test non-perturbative effects of the strong interaction, without perturbative contaminations. The perturbative corrections induced by the non-zero quark masses are tiny and can be easily taken into account. In Eq. (2) we have made explicit the contribution of the pion pole to the longitudinal axial-vector two-point function. We will work in the isospin limit $m_u = m_d \equiv m_q$ where the longitudinal part of the vector correlator vanishes.

The correlator $\overline{\Pi}(s)$ is analytic in the entire complex s plane, except for a cut on the positive real axis that starts at the threshold $s_{\rm th} = 4m_\pi^2$. Applying Cauchy's theorem in the

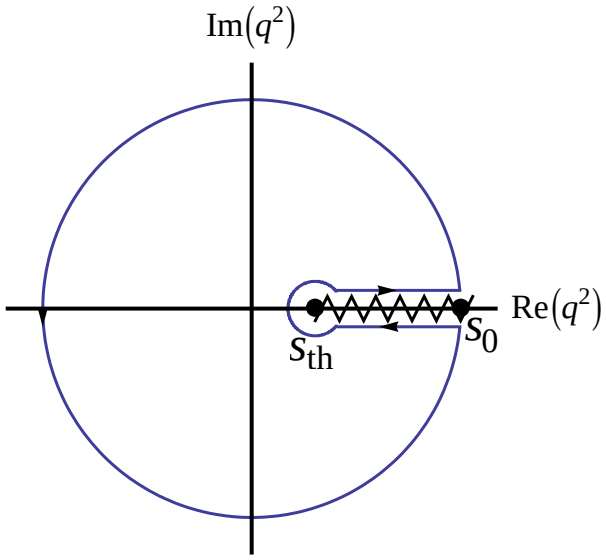

Figure 1: Analytic structure of $\overline{\Pi}(s)$.

circuit in Fig. 1 to the function $\omega(s)\,\Pi(s)$, one gets the exact expression [24]:

$$\int_{s_{\rm th}}^{s_0} ds\;\omega(s)\,\frac{1}{\pi}\,{\rm Im}\,\Pi(s) + \frac{1}{2\pi i}\oint_{|s|=s_0} ds\;\omega(s)\,\Pi(s) \;=\; 2\,f_\pi^2\,\omega(m_\pi^2) + {\rm Res}[\omega(s)\Pi(s), s=0]\,, \quad (3)$$

which relates the correlator in the Euclidean region, where it can be approximated by its short distance Operator Product Expansion (OPE) [31, 32],

$$\Pi^{\rm OPE}(s) \;=\; \sum_k \frac{\mathcal{O}_{2k}}{(-s)^k}\;, \quad (4)$$

with its imaginary part at Minkowskian momenta, accessible experimentally at low energies. For $s_{th} \leq s \leq m_\tau^2$, the spectral function $\rho(s) \equiv \frac{1}{\pi}\,{\rm Im}\,\Pi(s)$ is determined by the difference between the vector and axial-vector hadronic spectral functions measured in τ decays. Choosing different weight functions $\omega(s)$ one can change the sensitivity to different kinematical domains. We have only assumed that $\omega(s)$ is an arbitrary analytic function in the whole complex plane except maybe at the origin where it can have poles, generating the corresponding residue ${\rm Res}[\omega(s)\Pi(s), s=0]$. The pion pole contribution is given by the term $2f_\pi^2\,\omega(m_\pi^2)$.

The OPE expresses the correlator as an expansion in inverse powers of momenta, which approximates very well $\Pi(s)$ in the complex plane, away from the real axis, at large values of $|s|$. Therefore, it provides a very reliable short-distance tool to compute the integral along the circle $|s| = s_0$, for sufficiently large values of s_0. The main source of uncertainty is the integration region near the real axis, but it can be suppressed with adequately chosen weight functions [7]. In order to account for the small difference between the physical (exact) correlator and its OPE representation along the circle integration [16, 23, 33–35], one can introduce the correction [23, 35, 36]:

$$\delta_{\rm DV}[\omega(s), s_0] \;\equiv\; \frac{1}{2\pi i}\oint_{|s|=s_0} ds\;\omega(s)\;\left[\Pi(s) - \Pi^{\rm OPE}(s)\right] \;=\; \int_{s_0}^{\infty} ds\;\omega(s)\,\rho(s)\,, \quad (5)$$

which becomes zero at $s_0 \to \infty$. A non-zero value of $\delta_{\rm DV}[\omega(s), s_0]$ signals a violation of quark-hadron duality in the spectral integration between $s_{\rm th}$ and s_0. We will discuss later the best strategy to control and minimize this kind of theoretical uncertainty.

Taking $\omega(s) = s^n$ with non-negative values of the integer power n, the pion pole is the only singularity within the contour. Therefore, the integral over the spectral function from $s_{\rm th}$ to s_0 is equal to the pion pole term $2f_\pi^2 m_\pi^{2n}$, plus the OPE contribution $(-1)^n \mathcal{O}_{2(n+1)}$ generated by the integration along the circle, up to duality violations (DV). However, in the chiral limit ($m_q = 0$) and owing to the short-distance properties of QCD, $\Pi^{\rm OPE}(s)$ contains only power-suppressed terms from dimension $d = 2k$ operators, starting at $d = 6$ [37], which implies a vanishing OPE contribution for $n = 0, 1$:

$$\int_{s_{\rm th}}^{s_0} ds\, \frac{1}{\pi}\, {\rm Im}\, \Pi(s) \;=\; 2f_\pi^2 \,-\, \delta_{\rm DV}[1, s_0]\,, \tag{6}$$

$$\int_{s_{\rm th}}^{s_0} ds\, s\, \frac{1}{\pi}\, {\rm Im}\, \Pi(s) \;=\; 2f_\pi^2 m_\pi^2 \,-\, \delta_{\rm DV}[s, s_0]\,. \tag{7}$$

The superconvergence properties of $\Pi(s)$ guarantee that the DV corrections to both sum rules approach zero very fast for increasing values of s_0. When $s_0 \to \infty$, there is no duality violation and one gets the well-known first and second Weinberg Sum Rules (WSRs) satisfied by the physical spectral functions [38]. With non-zero quark masses taken into account, the first relation is still exact, while the second gets a negligible correction of $\mathcal{O}(m_q^2)$.

For higher values of the power n, Eq. (3) gives relations involving the different OPE coefficients:

$$\int_{s_{\rm th}}^{s_0} ds\, s^n\, \frac{1}{\pi}\, {\rm Im}\, \Pi(s) \;=\; (-1)^n\, \mathcal{O}_{2(n+1)} \,+\, 2f_\pi^2 m_\pi^{2n} \,-\, \delta_{\rm DV}[s^n, s_0] \qquad\qquad (n \geq 2)\,. \tag{8}$$

For negative values of $n = -m < 0$, the OPE does not give any contribution to the integration along the circle $s = s_0$, but there is a non-zero residue at the origen proportional to the $(m-1)$th derivative of $\overline{\Pi}(s)$ at $s = 0$. At low values of s the correlator can be rigorously calculated within chiral perturbation theory (χPT) [39–43]. At present $\Pi(s)$ is known to $\mathcal{O}(p^6)$ [44], in terms of the so-called chiral low-energy couplings (LECs) that we can determine through the relations:

$$\begin{aligned}\int_{s_{\rm th}}^{s_0} ds\, s^{-1}\, \frac{1}{\pi}\, {\rm Im}\, \Pi(s) \;&=\; 2\,\frac{f_\pi^2}{m_\pi^2} \,+\, \Pi(0) \,-\, \delta_{\rm DV}[s^{-1}, s_0] \\ &\equiv\; -8\, L_{10}^{\rm eff} \,-\, \delta_{\rm DV}[s^{-1}, s_0]\,,\end{aligned} \tag{9}$$

$$\begin{aligned}\int_{s_{\rm th}}^{s_0} ds\, s^{-2}\, \frac{1}{\pi}\, {\rm Im}\, \Pi(s) \;&=\; 2\,\frac{f_\pi^2}{m_\pi^4} \,+\, \Pi'(0) \,-\, \delta_{\rm DV}[s^{-2}, s_0] \\ &\equiv\; 16\, C_{87}^{\rm eff} \,-\, \delta_{\rm DV}[s^{-2}, s_0]\,.\end{aligned} \tag{10}$$

The explicit expression of the correlator $\overline{\Pi}(s)$ at $\mathcal{O}(p^6)$ in χPT is given in appendix A. The relation between the effective parameters $L_{10}^{\rm eff}$ and $C_{87}^{\rm eff}$ and their χPT counterparts, the LECs L_{10} and C_{87}, will be discussed in section 5.

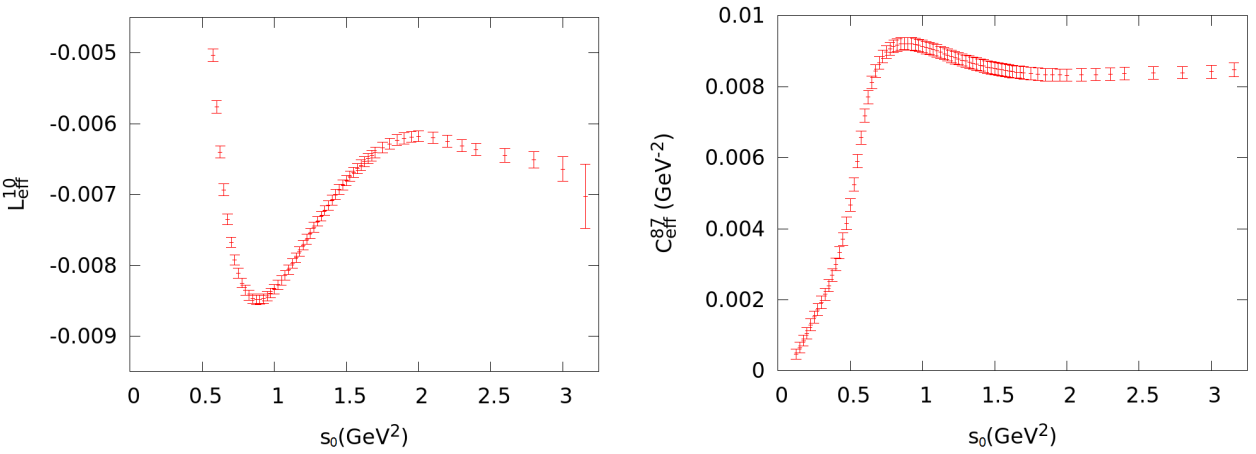

Figure 2: $L_{10}^{\rm eff}$ and $C_{87}^{\rm eff}$ from Eqs. (9) and (10), neglecting DVs, for different values of s_0.

2 A first estimation of the effective couplings

Using the updated ALEPH spectral function [29], we can determine $L_{10}^{\rm eff}$ and $C_{87}^{\rm eff}$ with Eqs. (9) and (10). As a first estimate, we neglect the DV terms and show in Fig. 2 the resulting effective couplings, for different values of s_0. As expected and as it was already observed in Ref. [22], the results exhibit a strong dependence on s_0 at low energies, where the duality-violation corrections are not negligible. At larger momentum transfers the curves start to stabilise, indicating that the violations of duality become smaller. However, especially for $L_{10}^{\rm eff}$, the curves are not yet horizontal lines at s_0 near m_τ^2, which implies that duality-violation effects are still present.

Instead of weights of the form s^n, we can try to reduce DV effects using pinched weight functions [7, 16, 45], which vanish at $s = s_0$ (or in the vicinity) where the OPE breaks down. Following Ref. [22], we employ the WSRs in Eqs. (6) and (7) and take $\omega_{-1,0}(s) = s^{-1}(1 - s/s_0)$ and $\omega_{-1}(s) = s^{-1}(1 - s/s_0)^2$ for estimating $L_{10}^{\rm eff}$, and $\omega_{-2,0}(s) = s^{-2}(1 - s^2/s_0^2)$ and $\omega_{-2}(s) = s^{-2}(1 - s/s_0)^2(1 + 2s/s_0)$ for estimating $C_{87}^{\rm eff}$. Again, neglecting the DV terms, we plot the values of the effective couplings for different s_0 in Fig. 3. We observe that using these pinched weights the results converge and become stable below $s = m_\tau^2$. This suggests that DV effects are negligible at $s_0 \sim m_\tau^2$, when these pinched weight functions are used. Assuming that, we obtain:

$$L_{10}^{\rm eff} = -(6.49 \pm 0.05) \cdot 10^{-3}\,, \tag{11}$$

$$C_{87}^{\rm eff} = (8.40 \pm 0.18) \cdot 10^{-3}\ \mathrm{GeV}^{-2}\,. \tag{12}$$

3 Dealing with violations of quark-hadron duality

The stability under changes of s_0 of the $L_{10}^{\rm eff}$ and $C_{87}^{\rm eff}$ determinations is a necessary condition for vanishing duality violations. However the plateau could be accidental and disappear at slightly higher values of s_0 where experimental data are not available. Although this

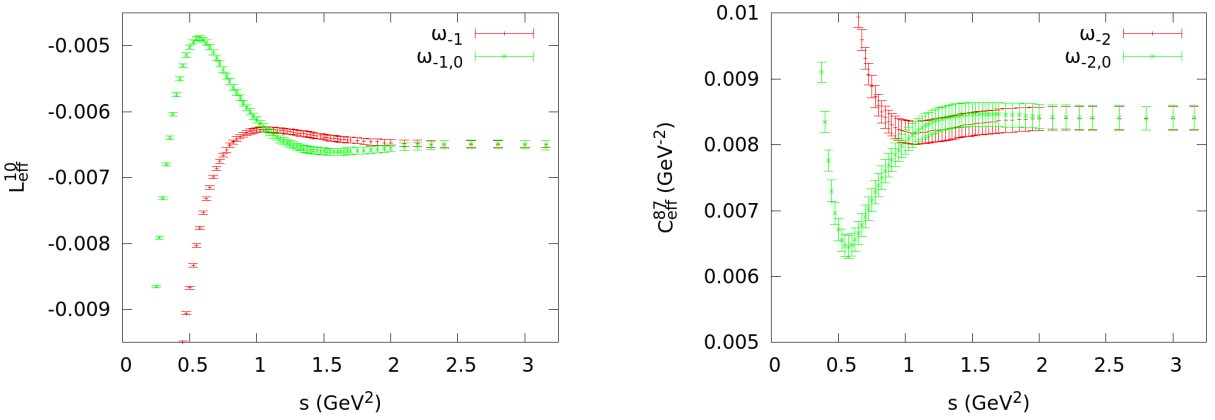

Figure 3: $L_{10}^{\rm eff}$ and $C_{87}^{\rm eff}$ at different values of s_0, using pinched weight functions and neglecting DVs.

possibility looks rather unlikely, we want to gain confidence on our numerical results and perform a reliable estimation of the uncertainties associated with violations of duality, using Eq. (5). The problem is that the spectral function is experimentally unknown above $s = m_\tau^2$.

Fortunately, there are strong theoretical constraints on $\rho(s)$ that originate in the special chiral-symmetry-breaking properties of $\Pi(s)$, implying its very fast fall-off at large momenta. In addition to the two WSRs, the spectral function should satisfy the so-called Pion Sum Rule (πSR), which determines the electromagnetic pion mass splitting in the chiral limit [46]:

$$\int_{s_{\rm th}}^{\infty} ds\; s\; \log\left(\frac{s}{\Lambda^2}\right)\; \frac{1}{\pi}\,{\rm Im}\,\Pi(s)\Big|_{m_q=0} \;=\; \left(m_{\pi^0}^2 - m_{\pi^+}^2\right)_{\rm em}\; \frac{8\pi}{3\alpha}\; f_\pi^2\big|_{m_q=0}\;. \tag{13}$$

Owing to the second WSR, the πSR does not depend on the arbitrary scale Λ. The r.h.s of this equation is well-known in χPT and, within the needed accuracy, we can identify in the l.h.s the spectral function in the chiral limit with the physical $\rho(s)$ because m_q corrections are tiny.

3.1 Parametrization of the spectral function

All the theoretical and phenomenological knowledge we have about $\Pi(s)$ can be used to get an estimate of the DV uncertainties. In order to do that, let us adopt the following ansatz for the spectral function at large values of s [23, 24, 47]:

$$\rho(s > s_z) \;=\; \kappa\, e^{-\gamma s}\, \sin\{\beta(s - s_z)\}\,, \tag{14}$$

with four free parameters κ, γ, β and s_z. This parametrization incorporates the expected strong fall-off when $s \to \infty$ and the oscillating behaviour predicted in resonance-based models [33,48,49]. We will split the spectral integrations in two parts, using the experimental data in the lower energy range and the ansatz (14) at higher energies. From the ALEPH data we know that the $V - A$ spectral function has a zero around $s_z \sim 2$ GeV^2, which is

represented in Eq. (14) through the s_z parameter. We will take this zero as the separation point between the use of the data and the use of the model.

Our parametrization is compatible with the ALEPH spectral function above s_z. Fitting the parameters given in (14) to the ALEPH data in the interval $s \in (1.7\ \text{GeV}^2, m_\tau^2)$, we obtain a very good fit with $\chi^2_{\text{min}}/\text{d.o.f.} = 8.52/9$. In fact, the fit with the updated ALEPH data looks more reliable compared to the previous one, where a value of $\chi^2_{\text{min}}/\text{d.o.f.} \ll 1$ was obtained [23].

We want to stress that the exact s-dependence of the spectral function in the high-energy region cannot be derived from first principles. The ansatz (14) is just a convenient parametrization, consistent with present knowledge, that we are going to use to estimate theoretical uncertainties associated with violations of quark-hadron duality. Imposing that $\rho(s)$ should satisfy all known theoretical and experimental constraints, the free parameters in the ansatz will allow us to measure how much freedom remains for the spectral function shape and, therefore, to obtain a reliable estimate of the associated uncertainty.

There is an inherent systematic error in any work that estimates DV effects, namely the dependence on the chosen parametrization. The comparison with other works that parametrize the data in a different way, such as Refs. [25, 27], represents an important step in this regard.

3.2 Selection of acceptable spectral functions

Following the procedure described in [23], we generate $3 \cdot 10^6$ tuples of the parameters $(\kappa, \gamma, \beta, s_z)$, randomly distributed in a rectangular region large enough to contain all the possible acceptable tuples. Among all generated tuples, we select those satisfying the following four physical conditions:

– The tuples must be consistent with the ALEPH data above $s = 1.7\ \text{GeV}^2$, *i.e.*, they must be contained within the 90% C.L. region in the fit to the experimental ALEPH spectral function described before:

$$\chi^2 \ < \ \chi^2_{\text{min}} \ + \ 7.78 \ = \ 16.30\,. \tag{15}$$

Although we will only use the ansatz above $s_z \sim 2\ \text{GeV}^2$, we impose the compatibility with the data from $1.7\ \text{GeV}^2$ to ensure the continuity of the spectral function in the matching region between the data and the model.

– The tuples must satisfy within the experimental uncertainties up to s_z the first and second WSRs with:

$$\int_0^{s_z} ds\ \rho(s)^{\text{ALEPH}} \ + \ \int_{s_z}^{\infty} ds\ \rho(s;\kappa,\gamma,\beta,s_z) \ = \ 17.0 \cdot 10^{-3}\,\text{GeV}^2\,, \tag{16}$$

$$\int_0^{s_z} ds\ s\ \rho(s)^{\text{ALEPH}} \ + \ \int_{s_z}^{\infty} ds\ s\ \rho(s;\kappa,\gamma,\beta,s_z) \ = \ 0.24 \cdot 10^{-3}\,\text{GeV}^4\,, \tag{17}$$

where the right-hand-side errors are omitted as they are negligible compared to the left-hand-side ones.

– The tuples must satisfy within the experimental uncertainties the πSR:

$$\int_0^{s_z} ds\ s\ \log\left(\frac{s}{1\text{GeV}^2}\right)\rho(s)^{\text{ALEPH}} \ + \ \int_{s_z}^{\infty} ds\ s\ \log\left(\frac{s}{1\text{GeV}^2}\right)\rho(s;\kappa,\gamma,\beta,s_z)$$
$$= \ -(10.9\pm 1.3)\cdot 10^{-3}\,\text{GeV}^4\,. \qquad (18)$$

The quoted error in the πSR takes into account that quark masses do not vanish in nature and we are using real data instead of chiral-limit one. We estimate this uncertainty taking for the pion decay constant the range $f_0 = (87 \pm 5)$ MeV [23], which includes the physical value and its estimated value in the chiral limit [50]. We also include a small uncertainty coming from the residual scale dependence of the logarithm, which is proportional to the second WSR.

We accept only those tuples that fulfil the four conditions. This requirement constrains the regions in the parameter space of the ansatz (14) that are compatible with both QCD and the data. From the initial set of $3 \cdot 10^6$ randomly generated tuples we obtain 3716 satisfying our set of minimal conditions. They represent the possible shapes of the spectral function beyond s_z, as shown in Fig. 4. In Fig. 5, we plot the statistical distribution of the parameters $(\kappa, \gamma, \beta, s_z)$ for the accepted tuples.

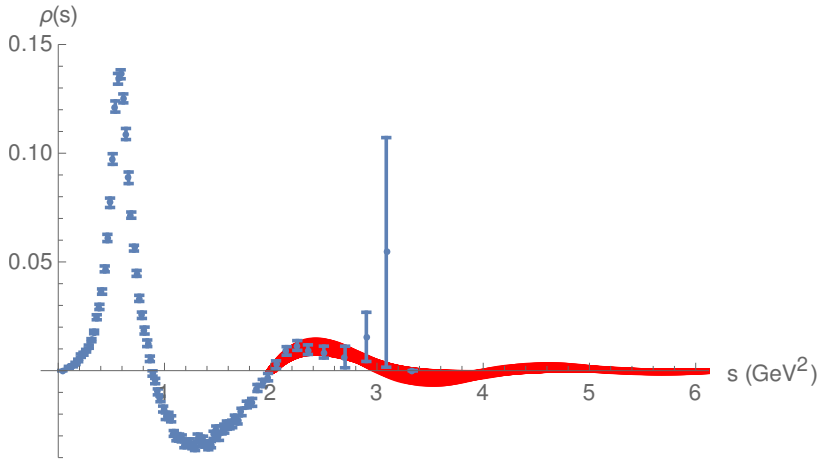

Figure 4: Updated ALEPH $V-A$ spectral function [29] (blue points) and all the "acceptable" spectral functions (red band above 1.7 GeV^2) that follow our parametrization and satisfy the physical conditions described in the main text.

4 Determination of physical parameters, including DV uncertainties

For every selected tuple we have an acceptable spectral function* that can be used to estimate the different physical parameters through the corresponding spectral integrals. Using

*Given by the ALEPH data below s_z and by the parametrization (14) above that value.

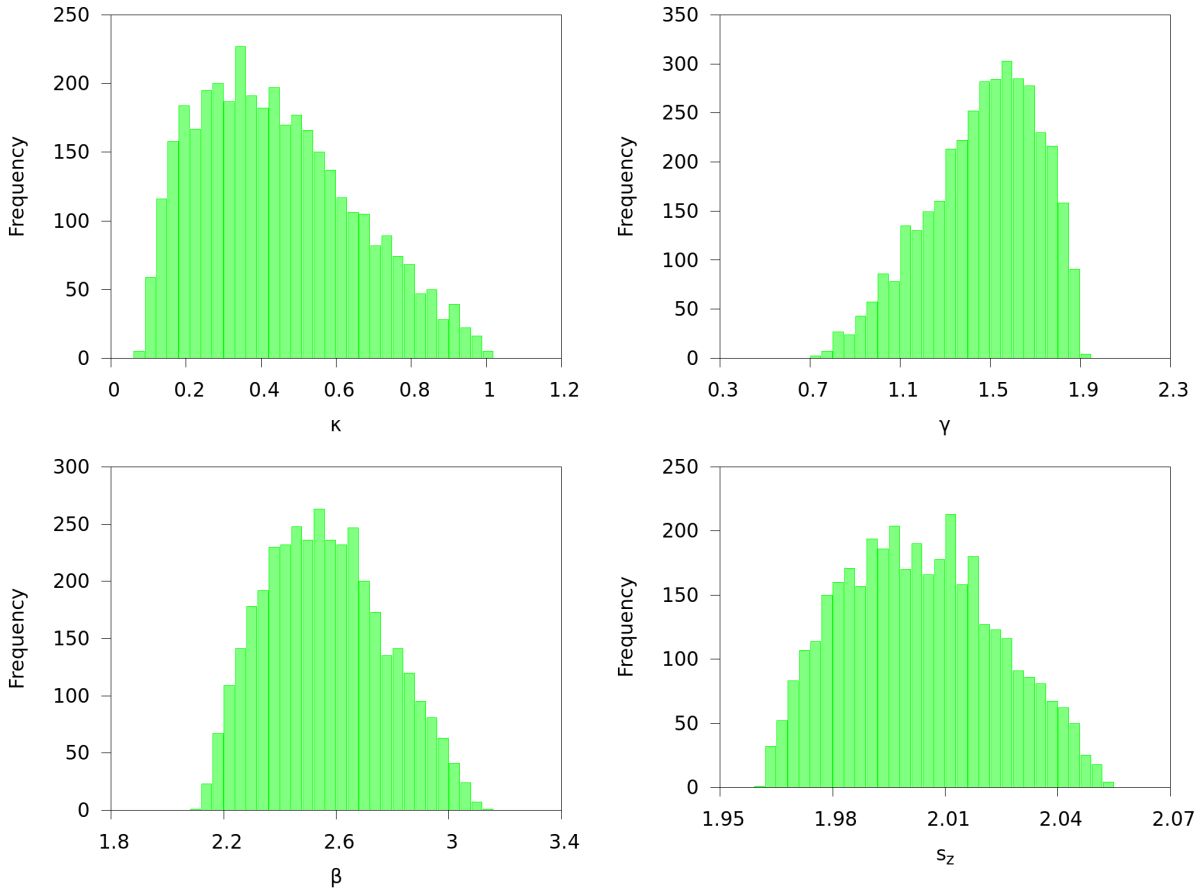

Figure 5: Distributions of the parameters (κ, γ, β, s_z) that satisfy the physical constraints. GeV units are used for dimensionful quantities.

Eqs. (9), (10) and (8) (for $n = 2, 3$) with $s_0 = s_z$, we determine $L_{10}^{\rm eff}$, $C_{87}^{\rm eff}$, $\mathcal{O}_6$ and $\mathcal{O}_8$ for each of the 3716 accepted tuples. The statistical distributions of the calculated parameters are shown in Fig. 6 (light gray).

We can reduce both the experimental and the DV uncertainties using the following pinched weight functions [24]:

$$\int_{s_{\rm th}}^{s_0} ds\, \frac{\rho(s)}{s^2}\left(1-\frac{s}{s_0}\right)^2\left(1+\frac{2s}{s_0}\right) = 16\,C_{87}^{\rm eff} - 6\,\frac{f_\pi^2}{s_0^2} + 4\,\frac{f_\pi^2 m_\pi^2}{s_0^3} - \delta_{\rm DV}[\omega_{-2}, s_0]\,, \tag{19}$$

$$\int_{s_{\rm th}}^{s_0} ds\, \frac{\rho(s)}{s}\left(1-\frac{s}{s_0}\right)^2 = -8\,L_{10}^{\rm eff} - 4\,\frac{f_\pi^2}{s_0} + 2\,\frac{f_\pi^2 m_\pi^2}{s_0^2} - \delta_{\rm DV}[\omega_{-1}, s_0]\,, \tag{20}$$

$$\int_{s_{\rm th}}^{s_0} ds\, \rho(s)\,(s-s_0)^2 = 2f_\pi^2 s_0^2 - 4f_\pi^2 m_\pi^2\, s_0 + 2f_\pi^2 m_\pi^4 + \mathcal{O}_6 - \delta_{\rm DV}[\omega_2, s_0]\,, \tag{21}$$

$$\int_{s_{\rm th}}^{s_0} ds\, \rho(s)\,(s-s_0)^2\,(s+2s_0) = -6f_\pi^2 m_\pi^2 s_0^2 + 4f_\pi^2 s_0^3 + 2f_\pi^2 m_\pi^6 - \mathcal{O}_8 - \delta_{\rm DV}[\omega_3, s_0]\,. \tag{22}$$

Following the same method with these relations, we obtain new distributions of acceptable

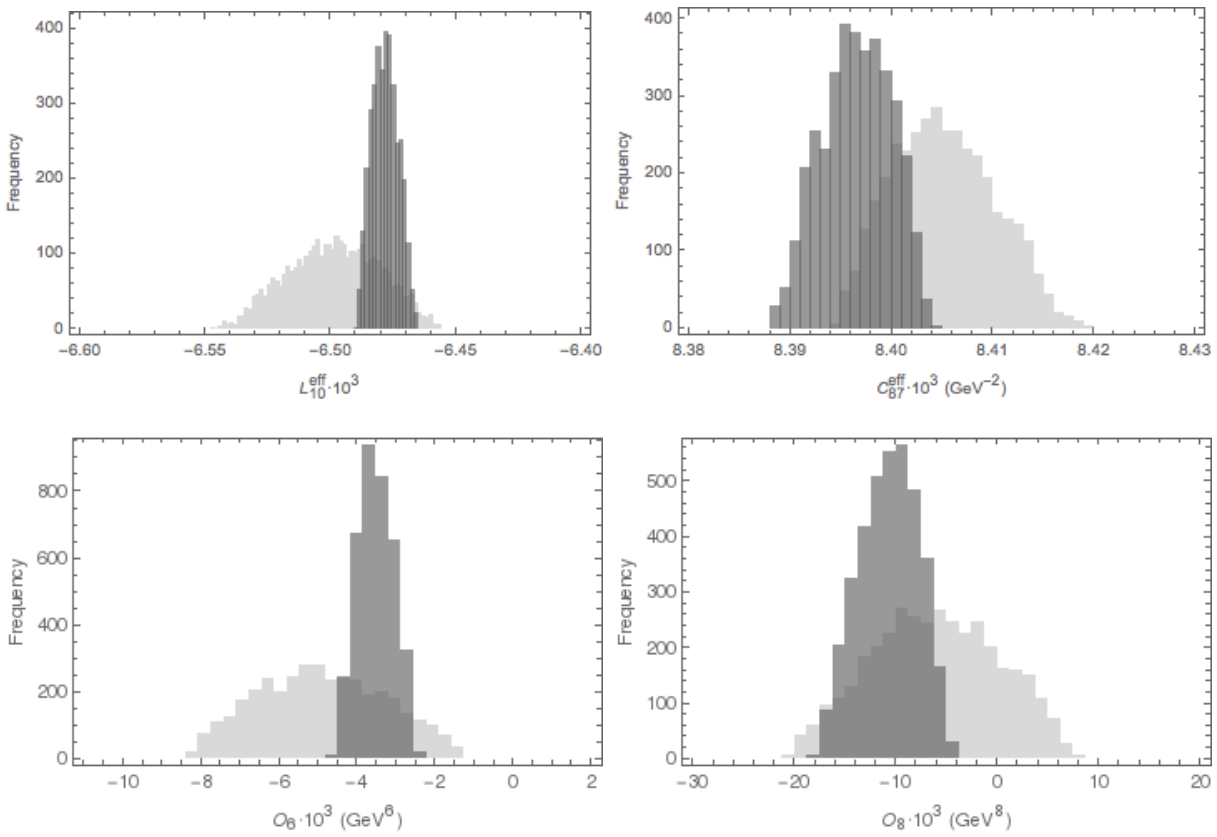

Figure 6: Statistical distribution of $L_{10}^{\rm eff}$, $C_{87}^{\rm eff}$, $\mathcal{O}_6$ y $\mathcal{O}_8$ for the tuples accepted, using s^n weights (light gray) and pinched weight (dark gray) functions.

physical parameters, which are also shown in Fig. 6 (dark gray). From these new distributions we get:

$$L_{10}^{\rm eff} = (-6.477\,^{+0.004}_{-0.006} \pm 0.05)\cdot 10^{-3} = (-6.48 \pm 0.05)\cdot 10^{-3}\,, \tag{23}$$

$$C_{87}^{\rm eff} = (8.399\,^{+0.002}_{-0.005} \pm 0.18)\cdot 10^{-3}\,{\rm GeV}^{-2} = (8.40 \pm 0.18)\cdot 10^{-3}\,{\rm GeV}^{-2}\,, \tag{24}$$

$$\mathcal{O}_6 = (-3.6\,^{+0.5}_{-0.4} \pm 0.5)\cdot 10^{-3}\,{\rm GeV}^6 = (-3.6\,^{+0.7}_{-0.6})\cdot 10^{-3}\,{\rm GeV}^6\,, \tag{25}$$

$$\mathcal{O}_8 = (-1.0 \pm 0.3 \pm 0.2)\cdot 10^{-2}\,{\rm GeV}^8 = (-1.0 \pm 0.4)\cdot 10^{-2}\,{\rm GeV}^8\,, \tag{26}$$

where the first errors correspond to DV uncertainties, computed from the dispersion of the histograms, and the second errors are the experimental ones.

We observe that pinched weight functions reduce indeed the DV effects, and that they are negligible for $L_{10}^{\rm eff}$ and $C_{87}^{\rm eff}$ at $s_0 \sim m_\tau^2$, compared with the experimental uncertainties. The results obtained for these two LECs are in perfect agreement with our first determinations in Eqs. (11) and (12) that did not include any estimate of DV. The corresponding spectral integrals contain weight functions with negative powers of s that suppress the contribution from the upper end of the integration range, making DV irrelevant. This is no-longer true for the vacuum condensates $\mathcal{O}_6$ and $\mathcal{O}_8$, which are determined with weight functions growing with positive powers of s. The use of pinched weights is then essential to suppress the

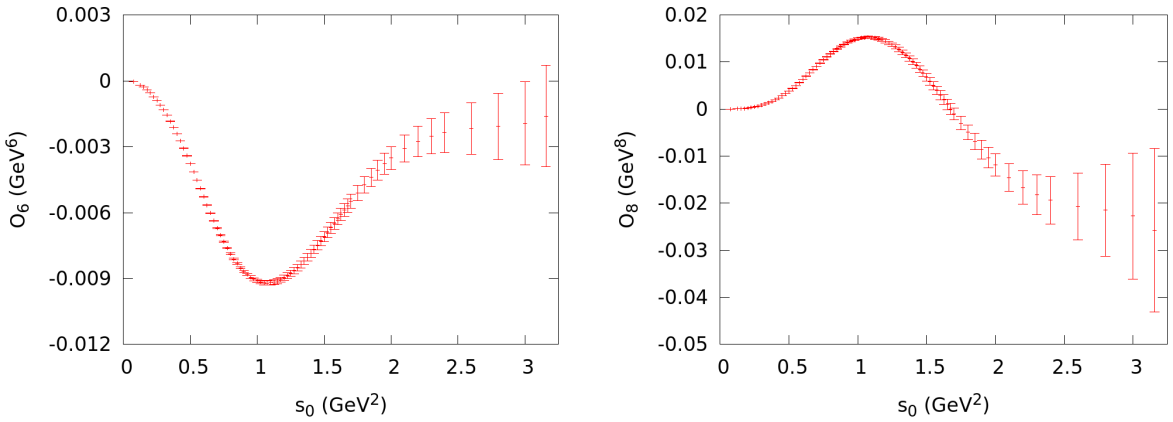

Figure 7: Values of the condensates $\mathcal{O}_6$ and $\mathcal{O}_8$, at different values of s_0, obtained from Eqs. (21) and (22) ignoring duality violations.

contributions from the region around s_0 in the contour integration. This is clearly reflected in the strong reduction of uncertainties observed in the two lower panels of Fig. 6.

Actually, ignoring completely DV effects, from the double-pinched weight functions in Eqs. (21) and (22) one obtains values for $\mathcal{O}_6$ and $\mathcal{O}_8$ that are perfectly compatible with our determinations in Eqs. (25) and (26), although with much larger experimental uncertainties. This is illustrated in Fig. 7, which shows how the extracted condensates stabilize at large s_0, around the right values but with very large error bars. The implementation of short-distance constraints (WSRs and πSR), through the procedure described in the previous section, has made possible to better pin down the spectral function in that region and obtain the more precise values in Eqs. (25) and (26).

Our results are in good agreement with those obtained previously in Ref. [24] with the 2005 ALEPH data set. Thus, the improvements incorporated in the 2014 release of the ALEPH data do not introduce sizeable modifications of the physical outputs. Similar results have been obtained recently in Ref. [27], using also the 2014 ALEPH data set.

Ref. [27] emphasises the existence of a slight tension with the results obtained in Ref. [25] with the 1999 OPAL data set [51]. In view of this, we have repeated our numerical analyses with the OPAL spectral function [51]. As happened with the 2005 ALEPH data set, the fit of the ansatz (14) to the OPAL data in the interval $s \in (1.7\ \text{GeV}^2, m_\tau^2)$ has a $\chi_{\rm min}/\text{d.o.f.} \ll 1$. Applying the same procedure used for ALEPH, we have obtained the following results with the OPAL data:

$$L_{10}^{\rm eff} = (-6.42 \pm 0.10) \cdot 10^{-3}\,, \tag{27}$$

$$C_{87}^{\rm eff} = (8.35 \pm 0.29) \cdot 10^{-3}\ \text{GeV}^{-2}\,, \tag{28}$$

$$\mathcal{O}_6 = (-5.7^{+1.1}_{-1.2}) \cdot 10^{-3}\ \text{GeV}^6\,, \tag{29}$$

$$\mathcal{O}_8 = (0.0^{+0.5}_{-0.6}) \cdot 10^{-2}\ \text{GeV}^8\,. \tag{30}$$

Owing to the larger uncertainties of the OPAL data, specially at higher values of s, the extracted parameters are less precise than those obtained with the ALEPH data. Neverthe-

less, comparing Eqs. (27)-(30) with (23)-(26), we observe a good agreement between both sets of results, the differences being only $0.5\,\sigma$, $0.1\,\sigma$, $1.6\,\sigma$ and $1.4\,\sigma$ for $L_{10}^{\rm eff}$, $C_{87}^{\rm eff}$, $\mathcal{O}_6$ and $\mathcal{O}_8$, respectively. We conclude that the much larger fluctuations obtained in Refs. [25, 27] between the results extracted from the two data sets are a consequence of the particular approach adopted in their DV analyses, which does not look optimal to us.[†]

Finally, we can use double-pinched weight functions in order to estimate higher-dimensional condensates:

$$\int_{s_{\rm th}}^{s_0} ds\; \rho(s)\; (s-s_0)^2\,(s^2+2s_0s+3s_0^2) \\ = \; -8f_\pi^2m_\pi^2s_0^3+6f_\pi^2s_0^4+2f_\pi^2m_\pi^8+\mathcal{O}_{10}-\delta_{\rm DV}[\omega_4,s_0]\,, \qquad (31)$$

$$\int_{s_{\rm th}}^{s_0} ds\; \rho(s)\; (s-s_0)^2\,(s^3+2s_0s^2+3s_0^2s+4s_0^3) \\ = \; -10f_\pi^2m_\pi^2s_0^4+8f_\pi^2s_0^5+2f_\pi^2m_\pi^{10}-\mathcal{O}_{12}-\delta_{\rm DV}[\omega_5,s_0]\,, \qquad (32)$$

$$\int_{s_{\rm th}}^{s_0} ds\; \rho(s)\; (s-s_0)^2\,(s^4+2s_0s^3+3s_0^2s^2+4s_0^3s+5s_0^4) \\ = \; -12f_\pi^2m_\pi^2s_0^5+10f_\pi^2s_0^6+2f_\pi^2m_\pi^{12}+\mathcal{O}_{14}-\delta_{\rm DV}[\omega_6,s_0]\,, \qquad (33)$$

$$\int_{s_{\rm th}}^{s_0} ds\; \rho(s)\; (s-s_0)^2\,(s^5+2s_0s^4+3s_0^2s^3+4s_0^3s^2+5s_0^4s+6s_0^5) \\ = \; -14f_\pi^2m_\pi^2s_0^6+12f_\pi^2s_0^7+2f_\pi^2m_\pi^{14}-\mathcal{O}_{16}-\delta_{\rm DV}[\omega_7,s_0]\,. \qquad (34)$$

Using these equations with the same method, we obtain from the ALEPH data:

$$\mathcal{O}_{10} \;=\; (5.6\pm1.2\pm0.8)\cdot10^{-2}\;{\rm GeV}^{10} \;=\; (5.6\pm1.4)\cdot10^{-2}\;{\rm GeV}^{10}\,, \qquad (35)$$

$$\mathcal{O}_{12} \;=\; (-0.13\,^{+\,0.01}_{-\,0.06}\pm0.02)\;{\rm GeV}^{12} \;=\; (-0.13\,^{+\,0.02}_{-\,0.07})\;{\rm GeV}^{12}\,, \qquad (36)$$

$$\mathcal{O}_{14} \;=\; (0.24\,^{+\,0.11}_{-\,0.05}\pm0.06)\;{\rm GeV}^{14} \;=\; (0.24\,^{+\,0.12}_{-\,0.08})\;{\rm GeV}^{14}\,, \qquad (37)$$

$$\mathcal{O}_{16} \;=\; (-0.38\,^{+\,0.25}_{-\,0.10}\pm0.13)\;{\rm GeV}^{14} \;=\; (-0.38\,^{+\,0.28}_{-\,0.17})\;{\rm GeV}^{16}\,. \qquad (38)$$

4.1 Comparison with previous works

Our final results for $L_{10}^{\rm eff}$, $C_{87}^{\rm eff}$, $\mathcal{O}_6$ and $\mathcal{O}_8$ are compared in Table 1 with recent (post-2005) phenomenological determinations of these parameters, obtained with different data

[†] In Refs. [25] and [27] the exact s-dependence of the resonance-based model (14) is assumed to be true for the V and A channels separately and a complex analysis involving 9 parameters, including a model-dependent determination of the strong coupling, is performed. In this way, uncertainties related to an α_s determination from the V and A spectral distributions are introduced in the analysis of the correlator $\Pi(s)$, which does not contain any perturbative contribution. Moreover the LECs and vacuum condensates are directly extracted from the fitted V and A spectral functions without imposing any further requirement (WSRs and πSR are only checked to be satisfied within errors a posteriori). Since DV is not very relevant for the extraction of the LECs, similar values are obtained for $L_{10}^{\rm eff}$ and $C_{87}^{\rm eff}$ with the two data sets. However, sizeable differences show up in their determinations of $\mathcal{O}_6$ and $\mathcal{O}_8$ where DV is more important.

$10^3 \cdot L_{10}^{\rm eff}$	$10^3 \cdot C_{87}^{\rm eff}$ (GeV^{-2})	$10^3 \cdot \mathcal{O}_6$ (GeV^6)	$10^2 \cdot \mathcal{O}_8$ (GeV^8)	Reference	Comments
-6.45 ± 0.06	–	-2.3 ± 0.6	-5.4 ± 3.3	BPDS'06 [19]	ALEPH'05 + DV=0
–	–	$-6.8\,^{+\,2.0}_{-\,0.8}$	$3.2\,^{+\,2.8}_{-\,9.2}$	ASS'08 [21]	ALEPH'05 + DV=0
-6.48 ± 0.06	8.18 ± 0.14	–	–	GPP'08 [22]	ALEPH'05 + DV=0
-6.44 ± 0.05	8.17 ± 0.12	-4.4 ± 0.8	-0.7 ± 0.5	GPP'10 [23, 24]	ALEPH'05 + DV_{V-A}
-6.45 ± 0.09	8.47 ± 0.29	-6.6 ± 1.1	0.5 ± 0.5	Boito'12 [25]	OPAL'99 + $\mathrm{DV}_{V/A}$
-6.50 ± 0.10	–	-5.0 ± 0.7	-0.9 ± 0.5	DHSS'15 [26]	ALEPH'14 + DV=0
-6.45 ± 0.05	8.38 ± 0.18	-3.2 ± 0.9	-1.3 ± 0.6	Boito'15 [27]	ALEPH'14 + $\mathrm{DV}_{V/A}$
-6.42 ± 0.10	8.35 ± 0.29	$-5.7\,^{+\,1.1}_{-\,1.2}$	$0.0\,^{+\,0.5}_{-\,0.6}$	this work	OPAL'99 + DV_{V-A}
-6.48 ± 0.05	8.40 ± 0.18	$-3.6\,^{+\,0.7}_{-\,0.6}$	-1.0 ± 0.4	this work	ALEPH'14 + DV_{V-A}

Table 1: Compilation of recent determinations of the LECs and vacuum condensates.

sets [28, 29, 51] and various DV parametrizations.[‡]

There is an excellent agreement among the different values quoted for the effective LECs $L_{10}^{\rm eff}$ and $C_{87}^{\rm eff}$, showing that these determinations are very solid and do not get affected by DV effects. In fact, as shown in Table 1, the precision has not changed in the last ten years. Nonetheless, the robustness of these determinations has increased significantly thanks to the thorough studies of DV effects with different approaches. The values obtained from different data sets are also in good agreement, although one can notice a $1\,\sigma$ shift of the $C_{87}^{\rm eff}$ central value when changing from the old (2005) to the updated (2014) ALEPH data.

The different results for $\mathcal{O}_6$ and $\mathcal{O}_8$ are also in reasonable agreement, within the quoted uncertainties. A good control of DV effects is more important for these vacuum condensates. The use of pinched weights allows to sizeably reduce their impact and obtain more reliable determinations. With the ALEPH'14 data one reaches a 20% accuracy for $\mathcal{O}_6$, but the error remains still large (40%) for $\mathcal{O}_8$. As commented before, we do not see any significant discrepancy between the results obtained from the OPAL and ALEPH data samples.

[‡]A complete list including theoretical estimates [52–54] and previous phenomenological determinations of these quantities (and of higher-dimensional condensates) [13–18, 20, 28, 34, 51, 55–59] can be found in Refs. [24, 60].

5 χPT couplings

The effective couplings $L_{10}^{\rm eff}$ and $C_{87}^{\rm eff}$ can be rewritten in terms of $\mathcal{O}(p^4)$ and $\mathcal{O}(p^6)$ couplings of the χPT Lagrangian [22, 44]:

$$\begin{aligned} L_{10}^{\rm eff} &\equiv -\frac{1}{8}\,\overline{\Pi}(0) \\ &= L_{10}^r(\mu) + \frac{1}{128\,\pi^2}\left[1 - \log\left(\frac{\mu^2}{m_\pi^2}\right) + \frac{1}{3}\,\log\left(\frac{m_K^2}{m_\pi^2}\right)\right] \\ &- \frac{1}{8}\,(\mathcal{C}_0^r + \mathcal{C}_1^r)\,(\mu) - 2\,(2\mu_\pi + \mu_K)\,(L_9^r + 2L_{10}^r)(\mu) + G_{2L}(\mu, s{=}0) + \mathcal{O}(p^8)\,, \quad (39) \end{aligned}$$

$$\begin{aligned} C_{87}^{\rm eff} &\equiv \frac{1}{16}\,\overline{\Pi}\,'(0) \\ &= C_{87}^r(\mu) - \frac{1}{64\,\pi^2 f_\pi^2}\left[1 - \log\left(\frac{\mu^2}{m_\pi^2}\right) + \frac{1}{3}\,\log\left(\frac{m_K^2}{m_\pi^2}\right)\right] L_9^r(\mu) \\ &+ \frac{1}{7680\,\pi^2}\left(\frac{1}{m_K^2} + \frac{2}{m_\pi^2}\right) - \frac{1}{2}\,G'_{2L}(\mu, s{=}0) + \mathcal{O}(p^8)\,, \quad (40) \end{aligned}$$

where the factors $\mu_i = m_i^2\log(m_i/\mu)/(16\pi^2 f_\pi^2)$ originate from one-loop corrections and $G_{2L}(\mu, s=0)$ and $G'_{2L}(\mu, s=0)$ are two-loop functions, whose numerical values are given in the appendix. We have also defined

$$\mathcal{C}_0^r = 32\,m_\pi^2\,(C_{12} - C_{61} + C_{80})\,, \quad (41)$$

$$\mathcal{C}_1^r = 32\,(m_\pi^2 + 2m_K^2)\,(C_{13} - C_{62} + C_{81})\,. \quad (42)$$

To first approximation the effective parameters correspond to the chiral couplings L_{10} and C_{87}, which appear at $\mathcal{O}(p^4)$ and $\mathcal{O}(p^6)$, respectively, in the χPT expansion. The scale dependence of $L_{10}^r(\mu)$ is cancelled by the one-loop logarithmic terms in the second line of Eq. (39), which are suppressed by one power of $1/N_C$ with respect to $L_{10}^r(\mu)$, where N_C is the number of QCD colours. The remaining contributions in Eq. (39) contain the $\mathcal{O}(p^6)$ corrections, which unfortunately introduce other $\mathcal{O}(p^6)$ and $\mathcal{O}(p^4)$ chiral couplings (third line). The corrections to $C_{87}^r(\mu)$ in Eq. (40) only involve one additional LEC, $L_9^r(\mu)$, through a one-loop correction with the $\mathcal{O}(p^4)$ chiral Lagrangian.

It is convenient to give the following compact numerical form of these equations to ease their future use:

$$L_{10}^{\rm eff} = L_{10}^r - 0.00126 + \mathcal{O}(p^6)\,, \quad (43)$$

$$L_{10}^{\rm eff} = 1.53\,L_{10}^r + 0.263\,L_9^r - 0.00179 - \frac{1}{8}\,(\mathcal{C}_0^r + \mathcal{C}_1^r) + \mathcal{O}(p^8)\,, \quad (44)$$

$$C_{87}^{\rm eff} = C_{87}^r + 0.296\,L_9^r + 0.00155 + \mathcal{O}(p^8)\,, \quad (45)$$

where we have used $\mu = M_\rho$ as the reference value for the χPT renormalization scale. The uncertainties in these numbers are much smaller than those affecting the different LECs and can therefore be neglected.

Working with $\mathcal{O}(p^4)$ precision, the determination of $L_{10}^r(\mu)$ is straightforward and we find:

$$L_{10}^r(M_\rho) \;=\; -(5.22 \pm 0.05) \cdot 10^{-3} \qquad\qquad [\mathcal{O}(p^4) \text{ analysis}]\,. \tag{46}$$

As mentioned before, an $\mathcal{O}(p^6)$ determination of L_{10}^r requires to know some next-to-next-to-leading-order (NNLO) LECs,[§] namely those in $\mathcal{C}_{0,1}^r$. This has motivated some interest in these quantities in the last few years. Here we briefly review the different approaches.

In the first $\mathcal{O}(p^6)$ determination of L_{10}^r [22], $\mathcal{C}_0^r$ was extracted from a combination of phenomenological ($C_{61,12}^r$) [62–65] and theoretical (C_{80}^r, RχT) [44, 66] inputs, namely[¶]

$$C_{61}^r(M_\rho) \;=\; (1.7 \pm 0.6) \cdot 10^{-3}\ \text{GeV}^{-2} \qquad [62, 64, 65]\,, \tag{47}$$

$$C_{12}^r(M_\rho) \;=\; (0.4 \pm 6.3) \cdot 10^{-5}\ \text{GeV}^{-2} \qquad [63]\,, \tag{48}$$

$$C_{80}^r(M_\rho) \;=\; (2.1 \pm 0.5) \cdot 10^{-3}\ \text{GeV}^{-2} \qquad [44, 66]\,, \tag{49}$$

whereas $\mathcal{C}_1^r$, which was completely unknown at the time, was estimated using

$$|C_{62}^r - C_{13}^r - C_{81}^r| \;\leq\; \frac{1}{3}\,|C_{61}^r - C_{12}^r - C_{80}^r|\,, \tag{50}$$

i.e., a simple educated guess based on the fact that those LECs are suppressed by a factor $1/N_C$. Using these numbers and Eq. (44), we obtain the results shown in Table 2 (5th row) and Fig. 8 (magenta point), which supersede those found in Ref. [22].

An alternative sum rule involving L_{10}^r and $\mathcal{C}_0^r$ was recently derived in Ref. [65] from an analysis of the flavour-breaking left-right correlator $\overline{\Pi}^{(0+1)}_{ud-us,LR}(0)$, namely[‖]

$$\begin{aligned}\left[\overline{\Pi}^{(0+1)}_{ud,LR}(0) - \overline{\Pi}^{(0+1)}_{us,LR}(0)\right]_{\text{LEC}} \;&=\; -0.7218\, L_5^r + 1.423\, L_9^r + 2.125\, L_{10}^r - \frac{m_K^2 - m_\pi^2}{m_\pi^2}\,\mathcal{C}_0^r \\ &=\; 0.0113\ (15)\,,\end{aligned} \tag{51}$$

again at $\mu = M_\rho$. Combining this constraint with the sum rule[**] in Eq. (44) and the naive inequality in Eq. (50), we obtain the results shown in Table 2 (6th row) and Fig. 8 (dark blue region). We see that L_{10}^r is in excellent agreement with the value obtained using Eqs. (47-49) and has a smaller error. Concerning the NNLO LECs, almost the same value is obtained for $\mathcal{C}_1^r$, whereas a 1.8 σ tension is present in the $\mathcal{C}_0^r$ case.

[§]It also requires L_9^r, which we take from Ref. [61]: $L_9^r(M_\rho) = 5.93\ (43) \cdot 10^{-3}$. Let us notice that this is the value used also in all other $\mathcal{O}(p^6)$ extractions of L_{10}^r from tau data.

[¶]This value of C_{61}^r comes from a flavour-breaking finite-energy sum rule involving the correlator $\overline{\Pi}^{(0+1)}_{ud-us,VV}(0)$. The original result [62] has been updated recently [65], finding

$$32\,(m_K^2 - m_\pi^2)\,C_{61} + 1.06\, L_{10}^r \;=\; 0.00727\ (134)\ .$$

Since L_{10}^r appears in this relation only at one loop, *i.e.* at $\mathcal{O}(p^6)$, we can use here an $\mathcal{O}(p^4)$ determination of L_{10}^r to extract C_{61}^r. We can indeed see that the L_{10}^r contribution to the C_{61}^r error is subdominant. We use the conservative value $L_{10}^r = -0.0052\ (17)$ to extract C_{61}^r.

[‖]We use the value obtained in Ref. [65] using 1999 OPAL data for the non-strange part, 0.0113 (15), instead of the more precise value of Ref. [27] from 2014 ALEPH data, 0.0111 (11), in order to avoid possible correlations with our determination of L_{10}^{eff}.

[**]We use $L_5^r(M_\rho) = (1.19 \pm 0.25) \cdot 10^{-3}$ [68] and, once again, $L_9^r(M_\rho) = 5.93\ (43) \cdot 10^{-3}$ [61].

$L_{10}^r(M_\rho)$ $\times 10^3$	$\mathcal{C}_0^r(M_\rho)$ $\times 10^3$	$\mathcal{C}_1^r(M_\rho)$ $\times 10^3$	Reference	Input
-4.06 (39)	+0.54 (42)	0 (5)	GPP'08 [22]	$\Pi(0) + \mathcal{C}_0^{\text{pheno/R}\chi\text{T}} + 1/N_c$
-3.10 (80)	-0.81 (82)	14 (10)	Boito'12 [25]	$\Pi(0) + \Pi(s)_{\text{latt}}$
-3.46 (32)	-0.34 (13)	8.1 (3.5)	Boyle'14, GMP'14 [65, 67]	$\Pi(0) + \Pi(s)_{\text{latt}} + \Delta\Pi(0)$
-3.50 (17)	-0.35 (10)	7.5 (1.5)	Boito'15 [27]	$\Pi(0) + \Pi(s)_{\text{latt}} + \Delta\Pi(0)$
-4.08 (44)	+0.21 (34)	0 (5)	this work	$\Pi(0) + \mathcal{C}_0^{\text{pheno/R}\chi\text{T}} + 1/N_c$
-4.17 (35)	-0.43 (12)	-1 (6)	this work	$\Pi(0) + \Delta\Pi(0) + 1/N_c$

Table 2: Compilation of recent determinations of the LECs. The determinations of L_{10}^{eff}, *i.e.* $\Pi(0)$, are obtained as explained in Table 1. $1/N_c$ refers to Eq. (50), whereas $\Delta\Pi(0)$ refers to the sum rule given in Eq. (51). Additional details are given in the text.

Another interesting development was performed in Ref. [67], where additional constraints on L_{10}^r, $\mathcal{C}_0^r$ and $\mathcal{C}_1^r$ were obtained from lattice simulations of the correlator $\overline{\Pi}(s)$ at unphysical meson masses. As shown in Table 2, the lattice data allow for a more accurate determination of the LECs, making unnecessary the use of the naive guess in Eq. (50). However, to derive the lattice constraints one needs to assume that the $\mathcal{O}(p^6)$ χPT expansion reproduces well the correlator at $s \sim -0.25\,\text{GeV}^2$, the energy region with smaller lattice uncertainties, which dominates these constraints. Unfortunately, it was shown in Ref. [25] that $\mathcal{O}(p^6)$ χPT does not approximate well enough $\overline{\Pi}(s)$ at these energies, taking into account the low uncertainties we are dealing with, and one needs to incorporate the so-far unknown $\mathcal{O}(p^8)$ chiral corrections.

In order to take advantage of the most precise lattice constraint, Ref. [27] makes the strong assumption that the missing $\mathcal{O}(p^8)$ chiral contributions are dominated by mass-independent terms, *i.e.*, $\overline{\Pi}(s) \approx \overline{\Pi}^{\chi\text{PT}}_{\mathcal{O}(p^6)} + D\,s^2$, so that they cancel in the lattice-continuum difference $\Pi^{\chi\text{PT}}_{\text{lattice}} - \Pi^{\chi\text{PT}}_{\text{physical}}$. It is worth noting that this is not a good approximation at the previous chiral order, $\mathcal{O}(p^6)$, since more than 25% of the $\mathcal{O}(p^6)$ correction proportional to s comes from known mass-dependent chiral terms. Therefore, the uncertainties associated with these lattice constraints seem at present underestimated.

Additionally, correlations between the continuum and the lattice sum rules (*e.g.* due to L_9^r) are not publicly available. It is worth mentioning nonetheless that if we implement these lattice constraints[††] (instead of the inequality in Eq. (50)), neglecting such correlations, we reproduce the results of Ref. [27] except for the uncertainties associated to L_5^r and L_9^r, for which the neglected correlations are likely to be relevant. Such an agreement is not surprising, as our determinations of the effective coupling L_{10}^{eff} were very close.

From Table 2 and Fig. 8 we see that the determinations obtained with the lattice constraints are (in most cases) significantly more precise than those using instead the inequality of Eq. (50). The agreement is reasonable (in the $0.5-1.7\,\sigma$ range depending on the quantity), taking into account that Eq. (50) is nothing but a naive educated guess, while the lattice

[††]We find that the constraint associated to the third lattice ensemble used in [27] fully dominates the fits.

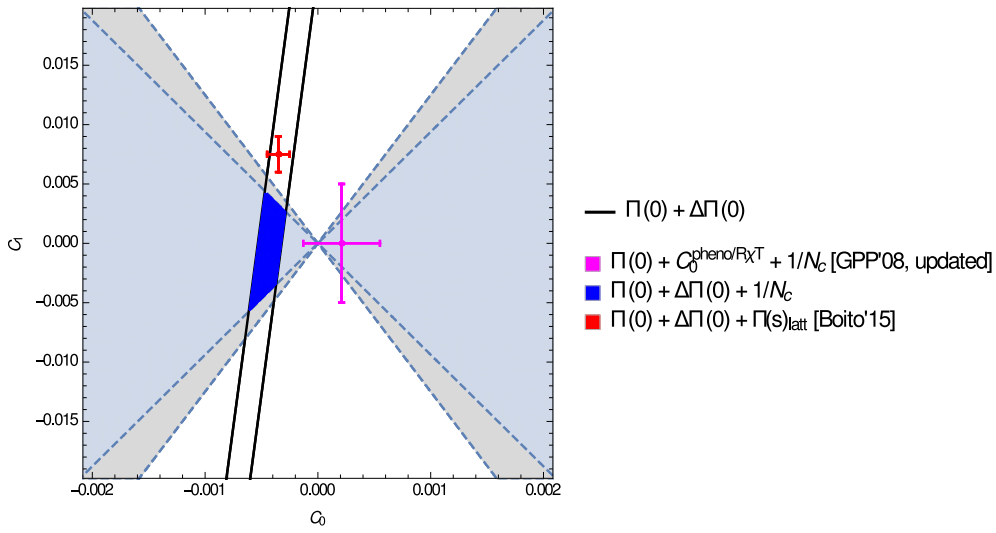

Figure 8: Latest determinations of the linear combinations of NNLO LECs $\mathcal{C}^r_{0,1}$, at $\mu = M_\rho$. We follow the same notation as in Table 2. The region allowed by the inequality of Eq. (50), inspired by large-N_c arguments, is indicated in light blue, whereas the light gray area around it (dashed) simply represents a naive estimate of its error, namely 33%.

improvement suffers from additional uncertainties not yet included in the quoted errors.

The determination of C^r_{87} from $C^{\rm eff}_{87}$ at $\mathcal{O}(p^6)$ does not involve any unknown LEC. The relation (40) contains a one-loop correction of size $-(3.16 \pm 0.13)\cdot 10^{-3}$, which only depends on $L^r_9(M_\rho)$ and the pion and kaon masses, and small non-analytic two-loop contributions collected in the term $G'_{2L}(M_\rho, s=0) = -0.28\cdot 10^{-3}\,\text{GeV}^{-2}$. In spite of its $1/N_C$ suppression, the one-loop correction is very sizeable, decreasing the final value of the $\mathcal{O}(p^6)$ LEC:

$$C^r_{87}(M_\rho) \;=\; (5.10 \pm 0.22)\cdot 10^{-3}\,\text{GeV}^{-2}\,. \tag{52}$$

5.1 Previous determinations with other methods

Our phenomenological determinations of $L^r_{10}(M_\rho)$ and $C^r_{87}(M_\rho)$ from τ decay data are in good agreement with the large-N_C estimates based on lowest-meson dominance [44, 69–73]:

$$\begin{aligned} L_{10} &= -\frac{F_V^2}{4M_V^2} + \frac{F_A^2}{4M_A^2} \approx -\frac{3f_\pi^2}{8M_V^2} \approx -5.4\cdot 10^{-3}\,, \\ C_{87} &= \frac{F_V^2}{8M_V^4} - \frac{F_A^2}{8M_A^4} \approx \frac{7f_\pi^2}{32M_V^4} \approx 5.3\cdot 10^{-3}\,\text{GeV}^{-2}\,. \end{aligned} \tag{53}$$

They also agree with the C_{87} determinations based on Pade approximants [53, 74], which are however unable to fix the renormalization-scale dependence that is of higher-order in $1/N_C$.

The resonance chiral theory (RχT) Lagrangian [70, 71, 75, 76] was used to analyze the left-right correlator at NLO in the $1/N_C$ expansion in Ref. [54]. Matching the effective field theory description with the short-distance QCD behavior, both LECs are determined,

keeping full control of their μ dependence. The predicted values [54]

$$\begin{aligned} L_{10}^r(M_\rho) &= -(4.4 \pm 0.9) \cdot 10^{-3}\,, \\ C_{87}^r(M_\rho) &= (3.6 \pm 1.3) \cdot 10^{-3}\ \text{GeV}^{-2}\,, \end{aligned} \tag{54}$$

are in good agreement with our determinations, although they are less precise.

Lattice determinations of the χPT LECs have improved considerably in recent times, although they are still limited to $\mathcal{O}(p^4)$ accuracy. The most recent simulations find:

$$L_{10}^r(M_\rho) \;=\; \left\{ \begin{array}{ll} -(5.7 \pm 1.1 \pm 0.7) \cdot 10^{-3} & [77]\,, \\ -(5.2 \pm 0.2\,^{+\,0.5}_{-\,0.3}) \cdot 10^{-3} & [78]\,. \end{array} \right. \tag{55}$$

These lattice results are in good agreement with our determinations, but their accuracy is still far from the phenomenological precision.

6 Conclusions

We have determined the LECs $L_{10}^{\rm eff}$ and $C_{87}^{\rm eff}$, using the recently updated ALEPH spectral functions [29], with the methods developed in Refs. [22–24]. Our final values, obtained using pinched weight functions with a statistical analysis that includes possible DV uncertainties, are:

$$L_{10}^{\rm eff} = (-6.48 \pm 0.05) \cdot 10^{-3}\,, \tag{56}$$

$$C_{87}^{\rm eff} = (8.40 \pm 0.18) \cdot 10^{-3}\ \text{GeV}^{-2}\,. \tag{57}$$

These results are in excellent agreement with the values extracted with non-pinched weights and with those determined neglecting DV in Eqs. (11) and (12). Thus, DV does not play any significant role in the determination of LECs, where the weight functions strongly suppress the high energy region of the spectral integrations. Our results are in good agreement with the ones obtained previously with the 2005 release of the ALEPH τ data [24]:

$$L_{10}^{\rm eff} = (-6.44 \pm 0.05) \cdot 10^{-3}\,, \tag{58}$$

$$C_{87}^{\rm eff} = (8.17 \pm 0.12) \cdot 10^{-3}\ \text{GeV}^{-2}\,. \tag{59}$$

The improvements introduced in the 2014 ALEPH data set did not bring major changes in these parameters. The values in Eqs. (56) and (57) also agree with the results obtained recently with the same experimental data but with a different approach in Ref. [27].

The statistical approach adopted in our analysis allows for a precise determination of the dimension-6 and 8 terms in the OPE of the left-right correlator $\Pi(s)$. We obtain:

$$\mathcal{O}_6 = (-3.6\,^{+\,0.7}_{-\,0.6}) \cdot 10^{-3}\ \text{GeV}^6\,, \tag{60}$$

$$\mathcal{O}_8 = (-1.0 \pm 0.4) \cdot 10^{-2}\ \text{GeV}^8\,, \tag{61}$$

also compatible with the determinations performed in Refs. [24] (with non-updated ALEPH data) and [27] (with a different approach for estimating DV effects). Using the same method, some higher-dimensional terms in the OPE have also being estimated in Eqs. (35)-(38).

The numerical determination of the effective couplings $L_{10}^{\rm eff}$ and $C_{87}^{\rm eff}$ has allowed us to derive the corresponding LECs of the χPT Lagrangian. At $\mathcal{O}(p^6)$, we find

$$L_{10}^r(M_\rho) = -(4.1 \pm 0.4) \cdot 10^{-3}\,, \tag{62}$$

$$C_{87}^r(M_\rho) = (5.10 \pm 0.22) \cdot 10^{-3}\,\text{GeV}^{-2}\,. \tag{63}$$

The final value quoted for $L_{10}^r(M_\rho)$ takes into account our two different estimates in Table 2, keeping conservatively the individual errors in view of the present uncertainties induced by the NLO LECs.

Acknowledgments

This work has been supported in part by the Spanish Government and ERDF funds from the EU Commission [Grants No. FPA2014-53631-C2-1-P and FPU14/02990], by the Spanish Centro de Excelencia Severo Ochoa Programme [Grant SEV-2014-0398] and by the Generalitat Valenciana [PrometeoII/2013/007]. M.G.-A. is grateful to the LABEX Lyon Institute of Origins (ANR-10-LABX-0066) of the Université de Lyon for its financial support within the program ANR-11-IDEX- 0007 of the French government.

A Low-energy expansion of the left-right correlation function

At low energies, the correlator $\Pi(s)$ can be expanded in powers of momenta over the chiral symmetry-breaking scale. The series expansion has been calculated to $\mathcal{O}(p^6)$ in χPT [40, 41, 44]:

$$\begin{aligned}
\Pi(s) &= \frac{2f_\pi^2}{s-m_\pi^2} - 8L_{10}^r - 8B_V^{\pi\pi}(s) - 4B_V^{KK}(s) \\
&+ 16\,C_{87}^r\,s \; - 32\,m_\pi^2\,(C_{61}^r - C_{12}^r - C_{80}^r) \\
&- 32\,(m_\pi^2 + 2m_K^2)\,(C_{62}^r - C_{13}^r - C_{81}^r) \\
&+ 16\left((2\mu_\pi + \mu_K)(L_9^r + 2L_{10}^r) - \left[2B_V^{\pi\pi}(s) + B_V^{KK}(s)\right]\,L_9^r\,\frac{s}{f_\pi^2}\right) \\
&- 8\,G_{2L}(s)\,,
\end{aligned} \tag{64}$$

where

$$B_V^{ii}(s) \equiv -\frac{1}{192\pi^2}\left(\sigma_i^2\left[\sigma_i\,\log\left(\frac{\sigma_i-1}{\sigma_i+1}\right)+2\right] - \log\left(\frac{m_i^2}{\mu^2}\right) - \frac{1}{3}\right)\,, \tag{65}$$

$$\sigma_i = \sqrt{1-\frac{4m_i^2}{s}}\,, \tag{66}$$

$$\mu_i \equiv m_i^2\log(m_i/\mu)/(16\pi^2 f_\pi^2)\,, \tag{67}$$

and $G_{2L}(s)$ is the two-loop contribution. The analytic expression of $G_{2L}(s)$ is too large to be given here, even in the $s \to 0$ limit; it can be extracted from Ref. [44]. For $\mu = M_\rho$, the numerical values for its contribution and its derivative at $s = 0$ are:

$$G_{2L}(0) = -0.53 \cdot 10^{-3} \,, \tag{68}$$

$$G'_{2L}(0) = -0.28 \cdot 10^{-3} \text{ GeV}^{-2} \,. \tag{69}$$

References

[1] Antonio Pich. Precision Tau Physics. *Prog. Part. Nucl. Phys.*, 75:41–85, 2014.

[2] Stephan Narison and A. Pich. QCD Formulation of the tau Decay and Determination of $\Lambda_{\rm MS}$. *Phys. Lett.*, B211:183, 1988.

[3] E. Braaten. QCD Predictions for the Decay of the tau Lepton. *Phys. Rev. Lett.*, 60:1606–1609, 1988.

[4] Eric Braaten. The Perturbative QCD Corrections to the Ratio R for tau Decay. *Phys. Rev.*, D39:1458, 1989.

[5] E. Braaten, Stephan Narison, and A. Pich. QCD analysis of the tau hadronic width. *Nucl. Phys.*, B373:581–612, 1992.

[6] F. Le Diberder and A. Pich. The perturbative QCD prediction to R_τ revisited. *Phys. Lett.*, B286:147–152, 1992.

[7] F. Le Diberder and A. Pich. Testing QCD with tau decays. *Phys. Lett.*, B289:165–175, 1992.

[8] Antonio Pich and Joaquim Prades. Perturbative quark mass corrections to the tau hadronic width. *JHEP*, 06:013, 1998.

[9] Antonio Pich and Joaquim Prades. Strange quark mass determination from Cabibbo suppressed tau decays. *JHEP*, 10:004, 1999.

[10] E. Gámiz, M. Jamin, A. Pich, J. Prades, and F. Schwab. Determination of m_s and $|V_{us}|$ from hadronic tau decays. *JHEP*, 01:060, 2003.

[11] Elvira Gámiz, Matthias Jamin, Antonio Pich, Joaquim Prades, and Felix Schwab. V_{us} and m_s from hadronic tau decays. *Phys. Rev. Lett.*, 94:011803, 2005.

[12] John F. Donoghue and Eugene Golowich. Chiral sum rules and their phenomenology. *Phys. Rev.*, D49:1513–1525, 1994.

[13] M. Davier, L. Girlanda, Andreas Hocker, and J. Stern. Finite energy chiral sum rules and tau spectral functions. *Phys. Rev.*, D58:096014, 1998.

[14] S. Peris, B. Phily, and E. de Rafael. Tests of large N_c QCD from hadronic tau decay. *Phys. Rev. Lett.*, 86:14–17, 2001.

[15] Johan Bijnens, Elvira Gámiz, and Joaquim Prades. Matching the electroweak penguins Q_7, Q_8 and spectral correlators. *JHEP*, 10:009, 2001.

[16] Vincenzo Cirigliano, Eugene Golowich, and Kim Maltman. QCD condensates for the light quark $V - A$ correlator. *Phys. Rev.*, D68:054013, 2003.

[17] C. A. Dominguez and K. Schilcher. Finite energy chiral sum rules in QCD. *Phys. Lett.*, B581:193–198, 2004.

[18] Stephan Narison. $V - A$ hadronic tau decays: A Laboratory for the QCD vacuum. *Phys. Lett.*, B624:223–232, 2005.

[19] Jose Bordes, Cesareo A. Dominguez, Jose Penarrocha, and Karl Schilcher. Chiral condensates from tau decay: A Critical reappraisal. *JHEP*, 02:037, 2006.

[20] A. A. Almasy, K. Schilcher, and H. Spiesberger. QCD condensates of dimension D=6 and D=8 from hadronic tau decays. *Phys. Lett.*, B650:179–184, 2007.

[21] A. A. Almasy, K. Schilcher, and H. Spiesberger. Determination of QCD condensates from tau-decay data. *Eur. Phys. J.*, C55:237–248, 2008.

[22] Martín González-Alonso, Antonio Pich, and Joaquim Prades. Determination of the Chiral Couplings L_{10} and C_{87} from Semileptonic Tau Decays. *Phys. Rev.*, D78:116012, 2008.

[23] Martín González-Alonso, Antonio Pich, and Joaquim Prades. Violation of Quark-Hadron Duality and Spectral Chiral Moments in QCD. *Phys. Rev.*, D81:074007, 2010.

[24] Martín González-Alonso, Antonio Pich, and Joaquim Prades. Pinched weights and Duality Violation in QCD Sum Rules: a critical analysis. *Phys. Rev.*, D82:014019, 2010.

[25] Diogo Boito, Maarten Golterman, Matthias Jamin, Kim Maltman, and Santiago Peris. Low-energy constants and condensates from the τ hadronic spectral functions. *Phys. Rev.*, D87(9):094008, 2013.

[26] C. A. Dominguez, L. A. Hernandez, K. Schilcher, and H. Spiesberger. Chiral sum rules and vacuum condensates from tau-lepton decay data. *JHEP*, 03:053, 2015.

[27] Diogo Boito, Anthony Francis, Maarten Golterman, Renwick Hudspith, Randy Lewis, Kim Maltman, and Santiago Peris. Low-energy constants and condensates from ALEPH hadronic τ decay data. *Phys. Rev.*, D92(11):114501, 2015.

[28] S. Schael et al. Branching ratios and spectral functions of tau decays: Final ALEPH measurements and physics implications. *Phys. Rept.*, 421:191–284, 2005.

[29] Michel Davier, Andreas Hoecker, Bogdan Malaescu, Chang-Zheng Yuan, and Zhiqing Zhang. Update of the ALEPH non-strange spectral functions from hadronic τ decays. *Eur. Phys. J.*, C74(3):2803, 2014.

[30] D. R. Boito, O. Cata, M. Golterman, M. Jamin, K. Maltman, J. Osborne, and S. Peris. Duality violations in tau hadronic spectral moments. *Nucl. Phys. Proc. Suppl.*, 218:104–109, 2011.

[31] Kenneth G. Wilson. Nonlagrangian models of current algebra. *Phys. Rev.*, 179:1499–1512, 1969.

[32] Mikhail A. Shifman, A.I. Vainshtein, and Valentin I. Zakharov. QCD and Resonance Physics. Theoretical Foundations. *Nucl. Phys.*, B147:385–447, 1979.

[33] Mikhail A. Shifman. Quark hadron duality. Eprint: hep-ph/0009131, 2000.

[34] Vincenzo Cirigliano, John F. Donoghue, Eugene Golowich, and Kim Maltman. Improved determination of the electroweak penguin contribution to ε'/ε in the chiral limit. *Phys. Lett.*, B555:71–82, 2003.

[35] O. Cata, M. Golterman, and S. Peris. Duality violations and spectral sum rules. *JHEP*, 0508:076, 2005.

[36] Boris Chibisov, R. David Dikeman, Mikhail A. Shifman, and N. Uraltsev. Operator product expansion, heavy quarks, QCD duality and its violations. *Int. J. Mod. Phys.*, A12:2075–2133, 1997.

[37] Claude W. Bernard, Anthony Duncan, John LoSecco, and Steven Weinberg. Exact Spectral Function Sum Rules. *Phys. Rev.*, D12:792, 1975.

[38] Steven Weinberg. Precise relations between the spectra of vector and axial vector mesons. *Phys. Rev. Lett.*, 18:507–509, 1967.

[39] Steven Weinberg. Phenomenological Lagrangians. *Physica*, A96:327, 1979.

[40] J. Gasser and H. Leutwyler. Chiral Perturbation Theory: Expansions in the Mass of the Strange Quark. *Nucl. Phys.*, B250:465, 1985.

[41] J. Gasser and H. Leutwyler. Low-Energy Expansion of Meson Form-Factors. *Nucl. Phys.*, B250:517–538, 1985.

[42] G. Ecker. Chiral perturbation theory. *Prog. Part. Nucl. Phys.*, 35:1–80, 1995.

[43] A. Pich. Chiral perturbation theory. *Rept. Prog. Phys.*, 58:563–610, 1995.

[44] Gabriel Amoros, Johan Bijnens, and P. Talavera. Two point functions at two loops in three flavor chiral perturbation theory. *Nucl. Phys.*, B568:319–363, 2000.

[45] C. A. Dominguez, L. A. Hernandez, K. Schilcher, and H. Spiesberger. Tau-decay hadronic spectral functions: probing quark-hadron duality. 2016. Eprint: arXiv:1602.00502, 2016.

[46] T. Das, G. S. Guralnik, V. S. Mathur, F. E. Low, and J. E. Young. Electromagnetic mass difference of pions. *Phys. Rev. Lett.*, 18:759–761, 1967.

[47] Oscar Cata, Maarten Golterman, and Santiago Peris. Possible duality violations in tau decay and their impact on the determination of α_s. *Phys. Rev.*, D79:053002, 2009.

[48] B. Blok, Mikhail A. Shifman, and Da-Xin Zhang. An Illustrative example of how quark hadron duality might work. *Phys. Rev.*, D57:2691–2700, 1998. [Erratum: Phys. Rev. D59, 019901 (1999)].

[49] Mikhail A. Shifman. Snapshots of hadrons or the story of how the vacuum medium determines the properties of the classical mesons which are produced, live and die in the QCD vacuum. *Prog. Theor. Phys. Suppl.*, 131:1–71, 1998.

[50] Sinya Aoki et al. Review of lattice results concerning low-energy particle physics. *Eur. Phys. J.*, C74:2890, 2014.

[51] K. Ackerstaff et al. Measurement of the strong coupling constant α_s and the vector and axial vector spectral functions in hadronic tau decays. *Eur. Phys. J.*, C7:571–593, 1999.

[52] Samuel Friot, David Greynat, and Eduardo de Rafael. Chiral condensates, Q_7 and Q_8 matrix elements and large-N_c QCD. *JHEP*, 10:043, 2004.

[53] Pere Masjuan and Santiago Peris. A Rational approach to resonance saturation in large-N_c QCD. *JHEP*, 05:040, 2007.

[54] A. Pich, I. Rosell, and J. J. Sanz-Cillero. Form-factors and current correlators: Chiral couplings $L^r_{10}(\mu)$ and $C^r_{87}(\mu)$ at NLO in $1/N_C$. *JHEP*, 07:014, 2008.

[55] R. Barate et al. Measurement of the spectral functions of axial - vector hadronic tau decays and determination of $\alpha_s(m^2_\tau)$. *Eur. Phys. J.*, C4:409–431, 1998.

[56] B. L. Ioffe and K. N. Zyablyuk. The $V-A$ sum rules and the operator product expansion in complex q^2 - plane from tau decay data. *Nucl. Phys.*, A687:437–453, 2001.

[57] B. V. Geshkenbein, B. L. Ioffe, and K. N. Zyablyuk. The Check of QCD based on the tau - decay data analysis in the complex q^2 - plane. *Phys. Rev.*, D64:093009, 2001.

[58] K. N. Zyablyuk. $V - A$ sum rules with $D = 10$ operators. *Eur. Phys. J.*, C38:215–223, 2004.

[59] Joan Rojo and Jose I. Latorre. Neural network parametrization of spectral functions from hadronic tau decays and determination of QCD vacuum condensates. *JHEP*, 01:055, 2004.

[60] Martín González-Alonso. *Low-energy tests of the Standard Model*. PhD thesis, University of Valencia, 2010.

[61] Johan Bijnens and P. Talavera. Pion and kaon electromagnetic form-factors. *JHEP*, 03:046, 2002.

[62] Stephan Durr and Joachim Kambor. Two point function of strangeness carrying vector currents in two loop chiral perturbation theory. *Phys. Rev.*, D61:114025, 2000.

[63] Matthias Jamin, Jose Antonio Oller, and Antonio Pich. Order p^6 chiral couplings from the scalar $K\pi$ form-factor. *JHEP*, 02:047, 2004.

[64] Karol Kampf and Bachir Moussallam. Tests of the naturalness of the coupling constants in ChPT at order p^6. *Eur. Phys. J.*, C47:723–736, 2006.

[65] Maarten Golterman, Kim Maltman, and Santiago Peris. NNLO low-energy constants from flavor-breaking chiral sum rules based on hadronic τ-decay data. *Phys. Rev.*, D89(5):054036, 2014.

[66] Rene Unterdorfer and Hannes Pichl. On the Radiative Pion Decay. *Eur. Phys. J.*, C55:273–283, 2008.

[67] P. A. Boyle, L. Del Debbio, N. Garron, R. J. Hudspith, E. Kerrane, K. Maltman, and J. M. Zanotti. Combined NNLO lattice-continuum determination of L^r_{10}. *Phys. Rev.*, D89(9):094510, 2014.

[68] R. J. Dowdall, C. T. H. Davies, G. P. Lepage, and C. McNeile. v_{us} from π and k decay constants in full lattice qcd with physical u, d, s and c quarks. *Phys. Rev.*, D88:074504, 2013.

[69] Marc Knecht and Andreas Nyffeler. Resonance estimates of $o(p^6)$ low-energy constants and qcd short distance constraints. *Eur. Phys. J.*, C21:659–678, 2001.

[70] V. Cirigliano, G. Ecker, M. Eidemuller, Roland Kaiser, A. Pich, and J. Portolés. Towards a consistent estimate of the chiral low-energy constants. *Nucl. Phys.*, B753:139–177, 2006.

[71] V. Cirigliano, G. Ecker, M. Eidemuller, A. Pich, and J. Portolés. The $\langle vap \rangle$ green function in the resonance region. *Phys. Lett.*, B596:96–106, 2004.

[72] A. Pich. Colorless mesons in a polychromatic world. In *Phenomenology of large-N_c QCD. Proceedings, Tempe, USA, January 9-11, 2002*, pages 239–258, 2002.

[73] Johan Bijnens and Gerhard Ecker. Mesonic low-energy constants. *Ann. Rev. Nucl. Part. Sci.*, 64:149–174, 2014.

[74] Pere Masjuan and Santiago Peris. A rational approximation to $\langle vv - aa \rangle$ and its $o(p^6)$ low-energy constant. *Phys. Lett.*, B663:61–65, 2008.

[75] G. Ecker, J. Gasser, H. Leutwyler, A. Pich, and E. de Rafael. Chiral lagrangians for massive spin 1 fields. *Phys. Lett.*, B223:425, 1989.

[76] G. Ecker, J. Gasser, A. Pich, and E. de Rafael. The role of resonances in chiral perturbation theory. *Nucl. Phys.*, B321:311, 1989.

[77] Peter A. Boyle, Luigi Del Debbio, Jan Wennekers, and James M. Zanotti. The s parameter in qcd from domain wall fermions. *Phys. Rev.*, D81:014504, 2010.

[78] E. Shintani, S. Aoki, H. Fukaya, S. Hashimoto, T. Kaneko, H. Matsufuru, T. Onogi, and N. Yamada. S-parameter and pseudo-nambu-goldstone boson mass from lattice qcd. *Phys. Rev. Lett.*, 101:242001, 2008.